Geologica Acta, Vol.16, Nº 4, December 2018, 499-518
DOI: 10.1344/GeologicaActa2018.16.4.10

geologica acta

Active fault control in the distribution of Elevated Low Relief Topography in the Central-Western Pyrenees

M. ORTUÑO[1] and M. VIAPLANA-MUZAS[2]

[1]Geomodels UB Research Institute and RISKNAT Group, Deptartament de Dinàmica de la Terra i de l'Oceà, Universitat de Barcelona
C/ de Martí i Franquès s/n, 08028 Barcelona, Spain. E-mail: maria.ortuno@ub.edu Phone: +34 93 402 13 78
Fax: +34 93 402 13 40

[2]Group of Dynamics of the Lithosphere (GDL), Institute of Earth Sciences Jaume Almera (ICTJA-CSIC)
C/ Lluís Solé i Sabarís s/n, 08028 Barcelona, Spain. E-mail: marc.via.mu@gmail.com

ABSTRACT

The activity of normal faults in the Central-Western Pyrenees is mainly detected by the disruption of paleic landforms surviving to Plio-Quaternary incision: the remnants of a Low-Relief Topography (LRT) that probably originated asynchronically during the Oligocene and Miocene. We propose a new method for mapping the LRT remnants that combines automatic analysis of digital topography and cross-checking with regional databases of Quaternary landforms. We focus on an area where the location of the main-drainage divide seems to be influenced by the activity of the Bedous-Pic de Midi du Bigorre set of faults and by the North Maladeta Fault. Neotectonic markers defined by the remnants of LRT envelops are tectonically displaced up to ~700m by the previously identified faults, but also along new faults observed in between them. A western prolongation of the North Maladeta Fault has been identified for the first time, implying a 75km total trace length, almost twice the previously published value. A restoration of the fault block motion was performed assuming a regional uplift across the range, enhanced in the northern part of the Axial Zone. This uplift leads to an outer arch extension along the Maladeta-Bedous Fault System. The resulting paleo-topography shows a broad southern paleo-flank (up to ~120km long) with a gentle regional gradient (~1º) and a much shorter and steeper northern paleo-flank (~4º gradient, up to 30km-long). This configuration suggests that the LRT remnants now located North of the main divide were connected to the Ebro Basin. The results are supported by previous studies on age and source provenance of major alluvial systems mantling the northern and southern flanks of the chain.

KEYWORDS | **Drainage divide. Neotectonics.Post-orogenic uplift. DEM analysis. Low Relief Topography (LRT).**

INTRODUCTION

Understanding the growth and decay of orogens through landscape evolution has interested and challenged scientists for many years (*e.g.* Davis, 1889; Penck, 1923; Birot, 1937; De Sitter, 1952; Kooi and Beaumont, 1989; Molnar and England, 1990). Flat-topped mountain ranges are controversial landforms analyzed in landscape evolution studies because their origin and preservation are not always straightforward (see Calvet *et al.*, 2015 for

discussion). The smooth or sub-horizontal remnants of erosive surfaces preserved at the highest parts of mountains are interpreted as the testimony of an ancient low relief landscape. These remnants, often called paleic surfaces, seem to be in most cases post-orogenic landforms because they bevel the contractional structures (*e.g.* Ollier and Pain, 2000; Calvet *et al.*, 2015). There is general agreement that these landforms are formed by slope reduction over long-periods (up to hundred to millions of years) when tectonics do not play a major controlling role in the macromorphology. This does not necessarily imply that tectonics are absent, but rather erosion predominates over tectonics, among a varied spectrum of interactions between factors such as deposition, isotactic uplift and subsidence (Phillips, 2002 and references therein). It is relevant to study the areas of elevated Low Relief Topography (henceforth LRT following the acronym proposed by Calvet and Gunnell *et al.*, 2008) in order to reconstruct the mountain building process because the generation and preservation of these areas must be consistent with the amounts of rock exhumation, the present-day activity of faults displacing these surfaces, and the evolution of the fluvial network. Two opposed models for explaining how flat top mountains are generated in orogens stand out today and can be seen as end members of a range of situations (Calvet *et al.*, 2015). The model most referred to is the *raised peneplain model*. Based on Davis's (1889) ideas on landscape cyclic evolution, these landforms are interpreted as resulting from the uplift of a former peneplain, which was generated at a lower altitude under the absence of tectonics. The model originally placed the paleo-base level near marine sea levels (*e.g.* Davis, 1911; De Sitter, 1952). Modern adaptations of this generation model, such as those proposed by Ollier and Pain (2000), Calvet and Gunnel (2008) and Farines *et al.* (2015), consider that the original paleo-base level did not necessarily correspond to a single marine base level, but that the base levels could have been multiple and temporally local rather than regional. Ollier and Pain (2000), among others, have found proposed a more gradual genesis of the low gradient topography, resulting from a balanced relationship between tectonics and erosion followed by uplift during the neotectonic period. The increase in altitude of the flat-tops of the mountains is frequently explained in relation to tectonic or isostatic uplift. This increase postdates the LRT completion and can be achieved by different processes. The Laramide ranges in the U.S.A. and the Quebrada del Toro Basin in the Argentinean Andes are two cases where the present-day altitudinal gradient between the relicts of peneplains and the original base level is unrealistically high or disrupted by surface deformation (Leonard, 2002; Hilley and Strecker, 2005).

At the opposite end of the spectrum of possible origins of LRT, there are researchers who believe that flat tops have not experienced any remarked uplift but rather were generated at an altitude similar to the present-day one in relation to a high base level. This model is called the *raised base level model*, as proposed by Babault *et al.* (2005). In this case, the raising of the base level occurs prior to surface completion, thus inhibiting incision. In the fluvio-alluvial systems draining into the mountain flanks, the base level, defined as the lower limit of an erosion process (Goudie, 2004), might be sea level, but also a lake water surface or a foreland basin overfilled with alluvial fans. In those cases, the apex of the fan, where the boundary between erosion and sedimentation is located, is considered the base level. The Altiplano and parts of the Tibetan plateau are considered modern analogues of peneplains generated at high altitude (Calvet *et al.*, 2015).

In the Pyrenees, remnants of LRT are preserved in the highest areas and the flanks of the range. These remnants can be studied to explore the long-term impact of post-orogenic active tectonics on the landscape configuration, a worldwide process that is difficult to study owing to the limited preservation of landforms in high mountain environments. The Pyrenean LRT remnants have been described over many years (Penck, 1885; Boissevain, 1934; Goron, 1937; Birot, 1937; García-Saínz, 1940; De Sitter, 1952; Peña, 1983; Rodríguez Vidal, 1983; Sala, 1984; among others). They have been systematically mapped along the Axial Zone (Babault *et al.*, 2005; Lynn, 2005; BRGM-IGME, 2009; Bosch, 2016; Bosch *et al.*, 2016a; Monod *et al.*, 2016) and in the Eastern Pyrenees (*e.g.* Calvet and Gunnel, 2008; Gunnel *et al.*, 2009). More local studies have focused on specific areas within the central parts of the range, such as the Aran valley (Kleinsmiede, 1960; Ortuño *et al.*, 2008, 2013), the Pallaresa valley (Zandvliet, 1960; Hartevelt, 1970) and other localities within the western part of the southernflank of the range (*e.g.* Barrere, 1962; Rodríguez-Vidal, 1983). The conception that the paleic smooth relief is composed of several generations of LRT remnants, as proposed for the Eastern Pyrenees by Calvet and Gunnell (2008) and Gunnell *et al.* (2008), has not been sufficiently explored in the Central-Western Pyrenees. Local cartographies performed in the 60's (Kleinsmiede, 1960; Zandvliet, 1960) distinguished two generations according to the relative height. Kleinmiede (1960) had already suggested that a third generation of lower surfaces observed in the Aran valley could have been downthrown by tectonic movements. The re-interpretation by Ortuño *et al.* (2008, 2013) of the LRT remnants in the Aran valley considers that the height different between those remnants is more likely explained by post-orogenic displacement along the North Maladeta Fault, affecting a single paleic surface pre-dating late Miocene. In the work by Bosch (2016), only one generation of paleic surfaces is envisaged across the chain, although a more recent completion is inferred for the western side. On the southern flank of

the Central-Western Pyrenees, Rodríguez Vidal (1983) identified upper, middle and lower generations of LRT remnants, and described tectonic displacement between the two higher ones. The relationship of these surfaces with underlying/overlying geological units allowed the author to interpret them as formed in the late Oligocene, late Miocene and Plio-Quaternary, respectively.

Independently of whether there is more than one generation, there is general agreement in recent works that the Pyrenean LRT remnants are post-orogenic landforms formed as the result of long-periods of mountain erosion. These works assign Oligocene–Miocene and post-middle Miocene to Quaternary ages to these remnants, depending on the locality and LRT generation (Rodríguez Vidal, 1983; Calvet and Gunnell, 2008; Gunnell *et al*., 2008; Ortuño *et al*., 2013; see discussion section for detailed ages). Nevertheless, there is no agreement about how they were generated and preserved, as detailed below in the following sub-section. Among the issues that have not been analyzed yet is the relationship between the position of the main-drainage divide of the range and the location of these surfaces. Has the position of the divide changed markedly since the LRT was originated? If so, how has it changed? Was it forced exclusively by slope movements and erosion? To answer these questions, it is necessary to review the geometry of the main divide considering active faults and fluvial-drainage configuration. The geometry of the main divide of the Pyrenees shows a marked kink in the middle of the chain, representing ~25km offset between the eastern and western-central segments (Fig. 1). This kink, analyzed in previous works, has been attributed to two main causes: i) The relatively northernmost position of resistant lithologies (crystalline massifs) in the eastern part of the chain (Lynn, 2005) and; ii) The larger erosive capacity of the northwestern rivers, resulting from an increased moisture supply from the Atlantic (Babault *et al*., 2011) and possibly related to their relatively shorter length, compared to rivers draining South (Struth and Teixell, 2016). These previous works did not discuss, however, the impact of active faults located near the divide. Faults such as the North Maladeta Fault (Ortuño *et al*., 2008, 2013) and the Bedous-Pic de Midi-Bigorreset of faults (Lacan, 2008; Dumont *et al*., 2015) are seismically active and located at less than 20km North of the main-drainage divide, which suggests that they have a possible control on drainage divide geometry. These faults have an E-W trend and show a ~60–70º dip to the North, with the hanging wall downthrown, as inferred from distribution of seismicity, geophysical, geomorphological and tectono-sedimentary data (Lacan, 2008; Ortuño, 2008; Ortuño *et al*., 2008, 2013; Dumont *et al*., 2015). Lacan and Ortuño (2012) and Dumont *et al*. (2015) proposed the possibility that local steepening of these vertical faults in the Axial Zone facilitates the present-day uplift of the Pyrenean core. Whichever have been the cause and the amount of uplift in the Axial Zone, these should be constrained in order to understand the evolution of the Pyrenean morphology.

In this paper, we study the LRT remnants preserved on both sides of a central section of the present-day main divide, where the position of the divide shows an abrupt kink. The study aims to understand: i) the origin of the LRT in the central part of the Pyrenees, to which no conclusive paleo-base level has been assigned to date and ii) the changes in the landscape following the generation of the LRT and how these could have been controlled by fault activity. By mapping and analyzing the ensemble of LRT remnants we aim to determine whether the paleo-surface envelope is valid as a neotectonic marker, which would provide insights into fault displacement along the active faults (Fig. 1). The LRT remnants and new faults have been identified through the analysis of Digital Elevation Models (DEM) of the present-day topography and satellite ortho-photographs and then cross-checking the observations and results in the field. The landscape preceding the fault activity was reconstructed using topographic sections and by considering the age and source provenance of the recent alluvial systems draining into the two foreland basins.

Axial Zone uplift and implications for LRT generation

The most controversial issue concerning the Pyrenean LRT remnants is the inference of their original altitude and the acceptance or rejection of posterior disruption by vertical movements. The first ideas about their origin (Goron, 1937; Birot, 1937) proposed that these surfaces were connected to marine sea levels before being uplifted. De Sitter (1952) correlated surfaces located between 1,000 and 2,000m-a.s.l. to assign an uplift of nearly 2km to the highest envelope of the Pyrenean peaks (located at 3,000m). The origin of raised peneplains was later supported in several studies that focused on the LRT remnants of the eastern (Calvet, 1992, 1996; Calvet and Gunnel, 2008; Gunnel *et al*., 2008, 2009) and central parts of the Pyrenees (Ortuño *et al*., 2013). In the Eastern Pyrenees, Calvet (1992, 1996, 1999) described vertical movements of the LRT remnants along post-orogenic faults. In subsequent studies combining geomorphological and structural data, provenance stratigraphy, biochronology and thermochronology (Calvet and Gunnel, 2008; Gunnel *et al*., 2008, 2009), two/three distinctive pulses of tectonic uplift (during Aquitanian-Burdigalian and after 12Ma, locally also during the Pliocene) were identified and it was found that they contributed to a regional uplift of ~2km. Gunnell *et al*. (2009) estimated the paleo-maximum altitude to be at the center of the range, at ~700–800m-a.s.l. Based on geophysical investigations, these authors proposed that the main driver of the post-orogenic uplift of the Eastern Pyrenees can be attributed to lithospheric thinning by thermal erosion.

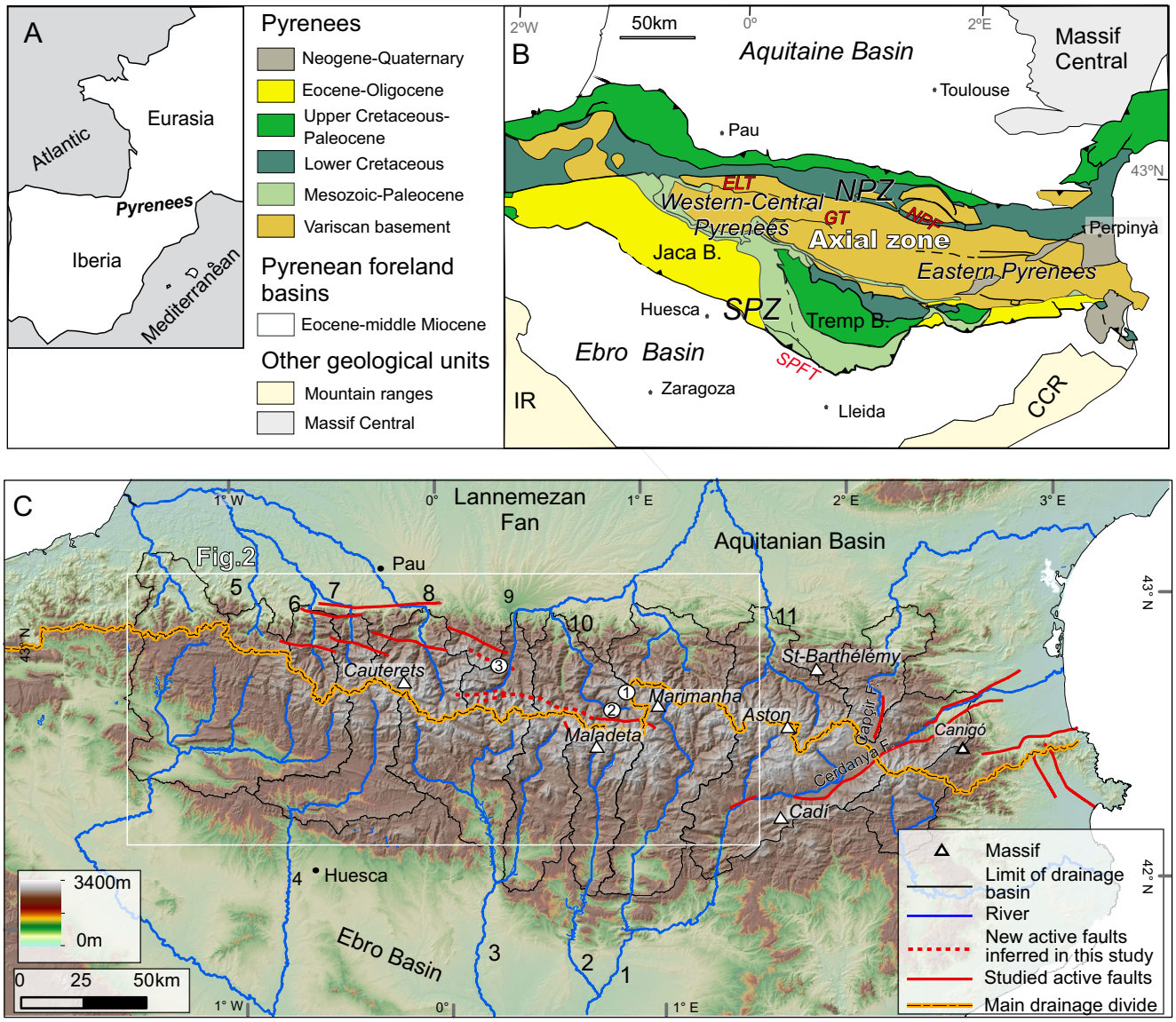

FIGURE 1. A) Location of the Pyrenees. B) Geological map of the Pyrenees and surrounding areas modified from Vergés *et al.* (2002). CCR: Catalan Coastal Ranges; ELT: Eaux Chaudes-Lakhoura Thrust; GT: Gavarnie Thrust; IR: Iberian Chain; NPF: North Pyrenean Fault; NPZ: North Pyrenean Zone; SPFT: South Pyrenean Frontal Thrust; SPZ: South Pyrenean Zone. C) Shaded relief map of the Pyrenees with the active faults and drainage divides; Non encircled numbers: rivers mentioned in the (1: Noguera Pallaresa; 2: Noguera Ribagorçana; 3: Cinca; 4: Aragon; 5: Saison; 6: Gave d'Aspe; 7: Gave d'Ossau; 9: Neste; 10: Garona; 11: Ariège). Encircled numbers: approximate localities showed in Figure 2 (1: Beret Plains and Liat Valley; 2: Aran Valley; 3: Portet de Louchon and Louron valleys).

However, the interpretation of the LRT remnants as an uplifted landform has been rejected by Babault *et al.* (2005), Bosch (2016) and Bosch *et al.* (2016a), who support a stagnant view of the relief and propose a *raised base level model* for the origin of these landforms. The model applied to the Pyrenees is inspired by the idea presented by Coney *et al.* (1996), who proposed a paleo-surface for the Pyrenean southern flank, existing in Oligocene–early Miocene times and extending from the Ebro Basin (500–700m) through the youngest southern syn-orogenic conglomerates, covering the southern part of the Axial Zone at 1,700–2,000m. They admitted that the original gradient of this surface is unknown, because the post-early Miocene uplift history of the Pyrenees is not well constrained. Among the main problems of this model, as considered by Calvet and Gunnell (2008) and Calvet *et al.* (2015), is that the present-day projected slope values between the Aquitaine Basin and the LRT remnants in the Axial Zone are between 3 and 4%, which is unrealistically high for a smooth relief. In addition, the proposed absence of uplift does not seem to be consistent with the isostatic response to a thinned crust, as inferred for the Eastern Pyrenees (Gunnel *et al.*, 2009).

METHODS

To achieve the study aim, we applied geomorphological and structural approaches with the following steps:

i) Identification of the LRT remnants in the Central-Western Pyrenees, focusing on the area where the divide shows an anomalous southern position;

ii) Characterization of these remnants according to their height, local relief and slope and the lithology on which they are developed. This last characteristic was obtained by surveying the 1:50,000 MAGNA geological maps of the Instituto Geológico y Minero de España (IGME, Geode; available in their web, see IGME (2018) for the link) and the french Bureau de Recherches Géologiques et Minières (BRGM, InfoTerre Portail; available in their web, see BRGM (2018) for the link);

iii) Analysis of topographic profiles to determine the variations in elevation of the LRT remnants across the active faults. The topographic profiles pass through the maximum number of remnants, drawing zigzagging curved traces. For the North Maladeta Fault, this step also led to reviewing the previously defined fault trace and detecting new fault branches. This was achieved by identifying marked offsets in the LRT remnants and the triangular facets associated with them. These features were mapped using a hill-shaded map derived from the 60m-DEM and by cross checking with Google Earth©. We also visited part of the area where new fault traces were detected;

iv) Restoration of the motion of the active faults and, afterwards, definition of the evolution of the land-surface from the late Oligocene to present. The paleo-relief was reconstructed using cross-sections perpendicular to the faults and along the maximum number of LRT remnants. Migration of the main-drainage was deduced by considering the highest areas after the retro-deforming of the remnants on both sides of the active faults, by accounting for the regional southern and northern paleo-slopes, and by cross-checking the results with source-provenance studies of alluvial fans preserved in the northern and southern flanks.

It is acknowledged that the LRT remnants that we observe today could have undergone land-lowering of up to dozens of meters, as inferred from 5 to 35mm/ka denudation rates derived from regolith development studies in the northern LRT remnants (Monod *et al.*, 2016). Denudation studies based on the concentration of cosmogenic nuclides performed by Crest (2017) point to erosion rates of between 10 and 40mm/ka that affect the elevated LRT remnants of the northern and eastern parts of the Pyrenees. With respect to the time frame, we assume a long time span (from late Oligocene to Pliocene) for the LRT completion in the study area. At the present stage of knowledge, we cannot tell whether these LRT remnants were part of a single generation of paleo-surface completed by the middle Miocene (Bosch, 2016) or late Miocene (Monod *et al.*, 2016;), or whether they belong to different generations, originated asynchronically and having contrasting ages.

Identification of paleo-low relief

To select areas of low relief preserved at high altitudes we applied a method inspired in previous approaches, such as those proposed by Babault *et al.* (2005), Calvet and Gunnell (2008) and Bosch (2016). The new method is adapted to automatically map a group of selected areas already identified manually as LRT remnants and combines automatic and manual steps described as follows:

Step 1. The preliminary identification was made through a combination of: i) inspection of Google Earth© 3D topography and satellite images (based on 60m-DEM); ii) inspection of 5m-DEM hill-shade maps (available: at www.ign.es/wmsinspire/) for the Spanish side and of 25m-DEM hill-shade maps generated from 25m-DEM (available at http://professionnels.ign.fr/) for the French side; iii) field cross checking at the headwaters of the Neste, Garona, and Pallaresa rivers. This step allowed us to estimate the approximate maximum value of the slope gradient of the most striking LRT remnants and the altitude under which the smooth topography most commonly corresponds to low lands developed in incised topography, such as planar valley floors. The parameters selected were 20º slope and 1,200m-altitude.

Step 2. Preliminary extraction of LRT remnants was performed using ArcGis© Spatial Analyst tools and considering the parameters previously selected. The DEM analyzed was the Aster GDem with a pixel size of 60m, so that all measurements yield a systematic error of 10–15m. Different values tested for slope and minimum height do not allow the main LRT identified in the field to be selected automatically for the entire area.

Step 3. Once the LRT remnants are automatically detected, the resulting polygons are filtered by crossing the map with the Quaternary Map of the Pyrenees (BRGM-IGME, 2009) to remove all patches of polygons interpreted as Quaternary landforms and to incorporate polygons located under 1,200m (all of them on the southern flank) and considered as LRT in this map.

Step 4. To calculate the local relief, understood as the difference between the higher altitude and the lower altitude within a pixel window, we used a pixel window with a radius of 500m.

Land-surface includes structural surfaces and depositional surfaces in the area connecting to the base level. Accordingly, we did not remove the structural surfaces and depositional surfaces when these matched the parameters selected to filter the topography (relief, slope and height). In this respect, the remnants should not be considered strictly erosional surfaces, but rather as belonging to a paleo-surface.

GEOLOGICAL SETTING

The Pyrenees are an Upper Cretaceous-Cenozoic collision orogen formed by the convergence of the Iberian and the Eurasian plates (Choukroune and Séguret, 1973). The structure of the chain results from the tectonic inversion of a Triassic–Cretaceous rift system and varies along the strike, showing maximum shortening in its central part (150km, ~40% shortening; Beaumont *et al*., 2000) and an over-imprint of Neogene extension in the eastern part (Gallart *et al*., 2001; Calvet and Gunell, 2008; Gunnell *et al*., 2009). The variations along and across the strike of the internal structure can be used to distinguish several parts within the Pyrenees; A major vertical structure, the North Pyrenean Fault (Fig. 1), separates the northern and southern sides of the orogen. In the proposed N-S structural sections (Muñoz, 1992; Teixell, 1998), the orogen shows an asymmetric distribution across the strike, where the northern part is vergent to the North and narrower with less accumulated shortening, and the southern part is South-vergent and much wider. In this paper, we distinguish the Eastern, Central-Western Pyrenees, and Western Pyrenees following a geological division. The two first regions coincide broadly with the geographical Pyrenees, whereas the Western Pyrenees (not shown in Fig. 1B) are commonly identified with the Cantabrian mountains and with the offshore part of the belt along the Bay of Biscay. The approximate limit between Eastern and Central-Western Pyrenees is at a longitude of ~1.5º (Fig. 1). The Eastern Pyrenees is affected by the Oligocene–Neogene Western Mediterranean extension, which extends to the West up to the Cerdanya (Roca, 1986) and Seu d'Urgell basins. In the Eastern and Central-Western Pyrenees, the orogen structure consists of a doubly vergent crustal wedge with a North Pyrenean thrust system (northward directed) and a South Pyrenean thrust system (southward directed), both involving Permian, Mesozoic and Cenozoic rocks (Fig. 1B; Muñoz, 2002). In the Central-Western Pyrenees, the basement located to the South of the North Pyrenean Zone is organized into an antiformal stack of three sheets, broadly coincident with the Axial Zone (Labaume *et al*., 2018; Muñoz, 1992, 2018; Teixell, 1998).

In this study, we focus on the geographical Pyrenees, which extend for nearly 450km, from the Gulf of Lion to the Bay of Biscay (Fig.1).The present-day fluvial network is mainly transversal (N-S), controlled by the regional slope of the mountain flanks; major river systems drain to the Ebro river (southern flank, connected to the Mediterranean Sea) and to the Garonne river (northern flank, connected to the Atlantic Ocean). Shorter rivers, however, flow directly to the Mediterranean Sea and the Atlantic Ocean (Fig. 1).

Timing of the orogenic growth

The growth of the Pyrenean orogenic belt, as inferred from the structural, thermo-chronological and source-provenance analysis of the southern and axial zones (*e.g*. Muñoz, 1992; Coney *et al*., 1996; Fitzgerald *et al*., 1999; Beaumont *et al*., 2000; Fidalgo-González, 2001; Beamud *et al*., 2003, 2011; Whitchurch *et al*., 2011; Rushlow *et al*., 2013), can be explained as resulting from six main geological stages that are markedly asynchronous along and across the chain. These geological stages can be summarized as: i) Onset of the orogeny as the inversion of a rift during the late Santonian (Late Cretaceous); ii) Diachronous exhumation of the basement rocks (from Late Cretaceous to late Eocene) from East to West and from North to South, recorded in the syn-orogenic deposits (Rushlow *et al*., 2013 and references therein); iii) Burial of the South Pyrenean fold-and-thrust belt by up to 2km of upper Eocene–Oligocene sediments and synchronous to the onset of out-of-sequence thrusts and back-thrusts in the southern Pyrenees (*e.g*. Vergés and Muñoz, 1990; Vergés, 1993; Vergés and Burbanck, 1996; Meigs and Burbanck, 1997); iv) Syn- to early post-orogenic acceleration of the orogen exhumation in late Oligocene–early Miocene times (according to Beamud *et al*., 2011; around 25–30Ma in the Central Pyrenees, by and according to Fillon and Van der Beck, 2012; 30–37Ma in the Central-Western Pyrenees); v) Diachronous end of orogenic contraction that took place in the middle Oligocene in the Eastern Pyrenees and in the early Miocene in the Central-Western Pyrenees (Vergés *et al*., 1995; Millán-Garrido *et al*., 2000; Teixell and Muñoz, 2000; Arenas *et al*., 2001; Oliva-Urcia *et al*., 2015; Teixell *et al*., 2016); vi) Post-orogenic stage of quiescence tectonics with local extensional faulting that mainly developed in the eastern part, linked to the opening of the late Oligocene-Neogene Western Mediterranean (*e.g*. Calvet, 1996, 1999). In the northern part of the Central-Western Pyrenees, some of the major thrusts are inverted as normal faults (Lacan, 2008; Ortuño, 2008; Ortuño *et al*., 2008, 2013; Lacan and Ortuño, 2012).

RESULTS: RECONSTRUCTION OF THE PRE-QUATERNARY PYRENEAN TOPOGRAPHY

New cartography of the LRT remnants in the Central-Western Pyrenees

The Pyrenean topography in the study area shows numerous patches of smooth relief located at or near the

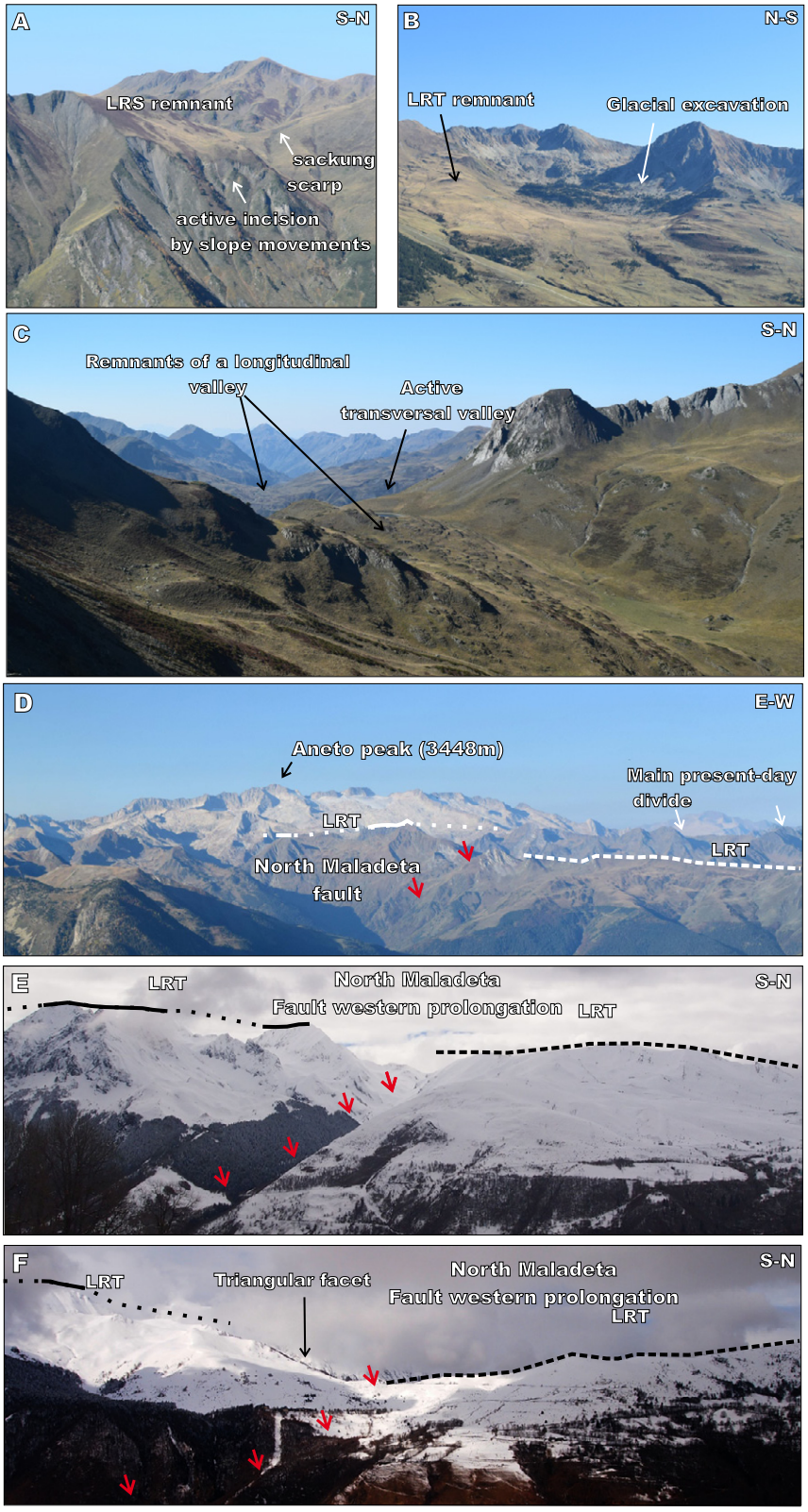

FIGURE 2. Photographs of the Central-Western Pyrenees illustrating the Low Relief Topography (LRT), the North Maladeta Fault and its western prolongation (Neste Fault). Location of the photographs sites is shown in Figure 1. A) Rock slope failures affecting LRT remnants at Liat valley; B) Glacial excavation of the LRT at Marimanha; C) Longitudinal paleo-valley deeply incised by the transversal Liat glacial valley at the Liat lacustrine area; D) Frontal view of the North Maladeta Fault and vertically displaced LTR surface and Aran Valley; E) View of the North Maladeta Fault western prolongation at the Portet de Louchon; E) View of the North Maladeta Fault western prolongation at the Louron Valley. Red arrows: location of the North Maladeta Fault; Solid white/black line: LRT remnant; Discontinuous white/black line: LRT interpolation.

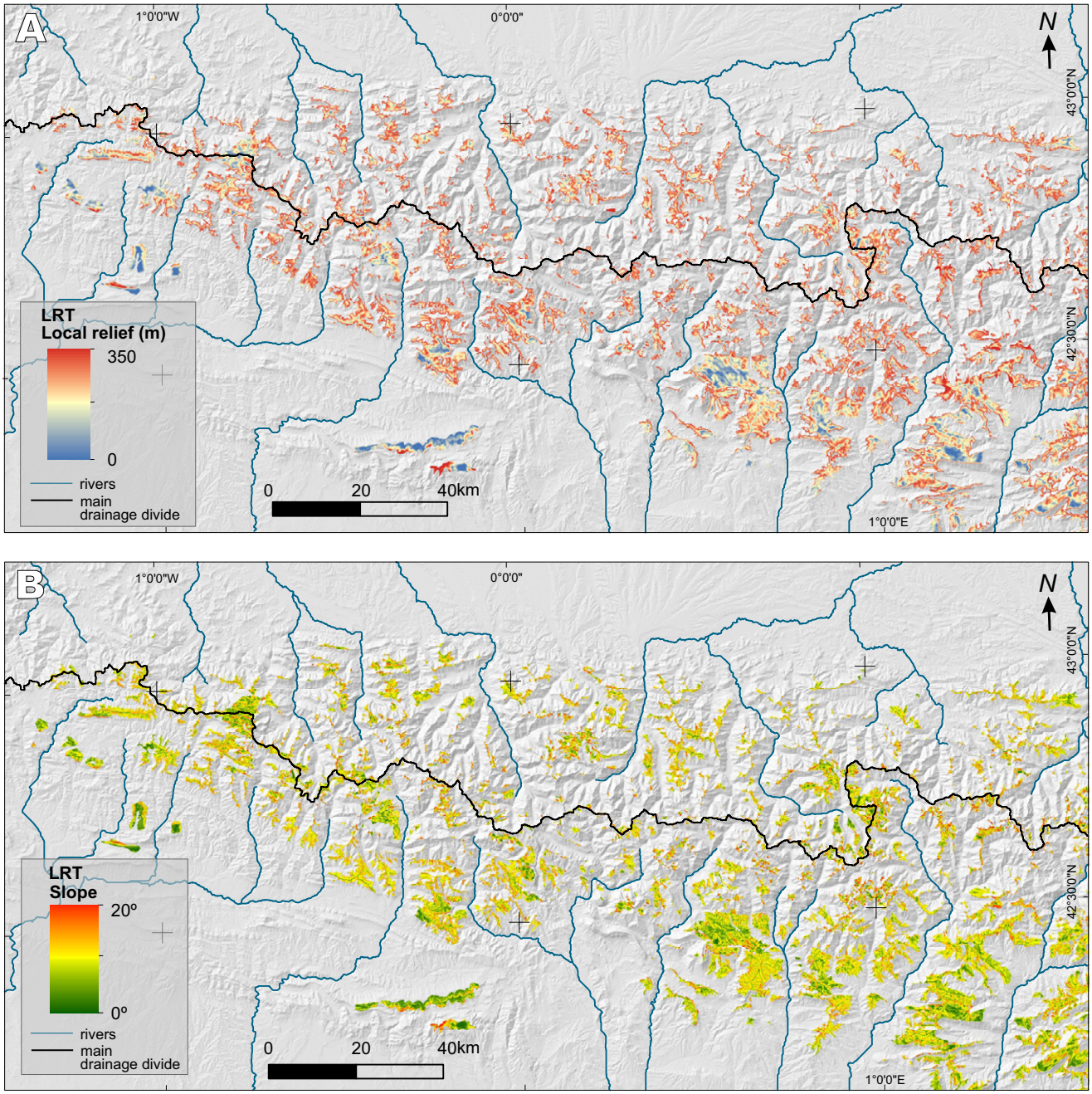

FIGURE 3. Shaded relief map (60m-DEM) of the Central-Western Pyrenees with the remnants of Low Relief Topography (LRT). A) Local relief of the LRT remnants. The relief is given for each pixel using a cell size of 500m. B) Slope of the LRT remnants.

water divides in summit positions (Figs. 2; 3; 4). The studied LRT remnant landforms generally have a regolith of variable thickness. This feature is not shared with the glaciated polish surfaces, which are also smooth high altitude landforms detected by the automatic procedure. The remnants are usually bounded and incised by rock slope failures; a characteristic that Jarman *et al.* (2014) and Calvet *et al.* (2015) also found in the Eastern Pyrenees (Fig. 2A). Some of the LRT display concave geometries at their boundaries, typical of a broad valley and suggesting they were part of a former-drainage system. At some sites, such as the Liat valley (Fig. 2C), the vestiges of this paleo-drainage are dissected by present-day orthogonal-drainage.

A few polygons (Fig. I Electronic Appendix, available at www.geologica-acta.com) were added to include areas located below 1,200m but that BRGM-IGME (2009) considered to be LRT remnants. These are located exclusively

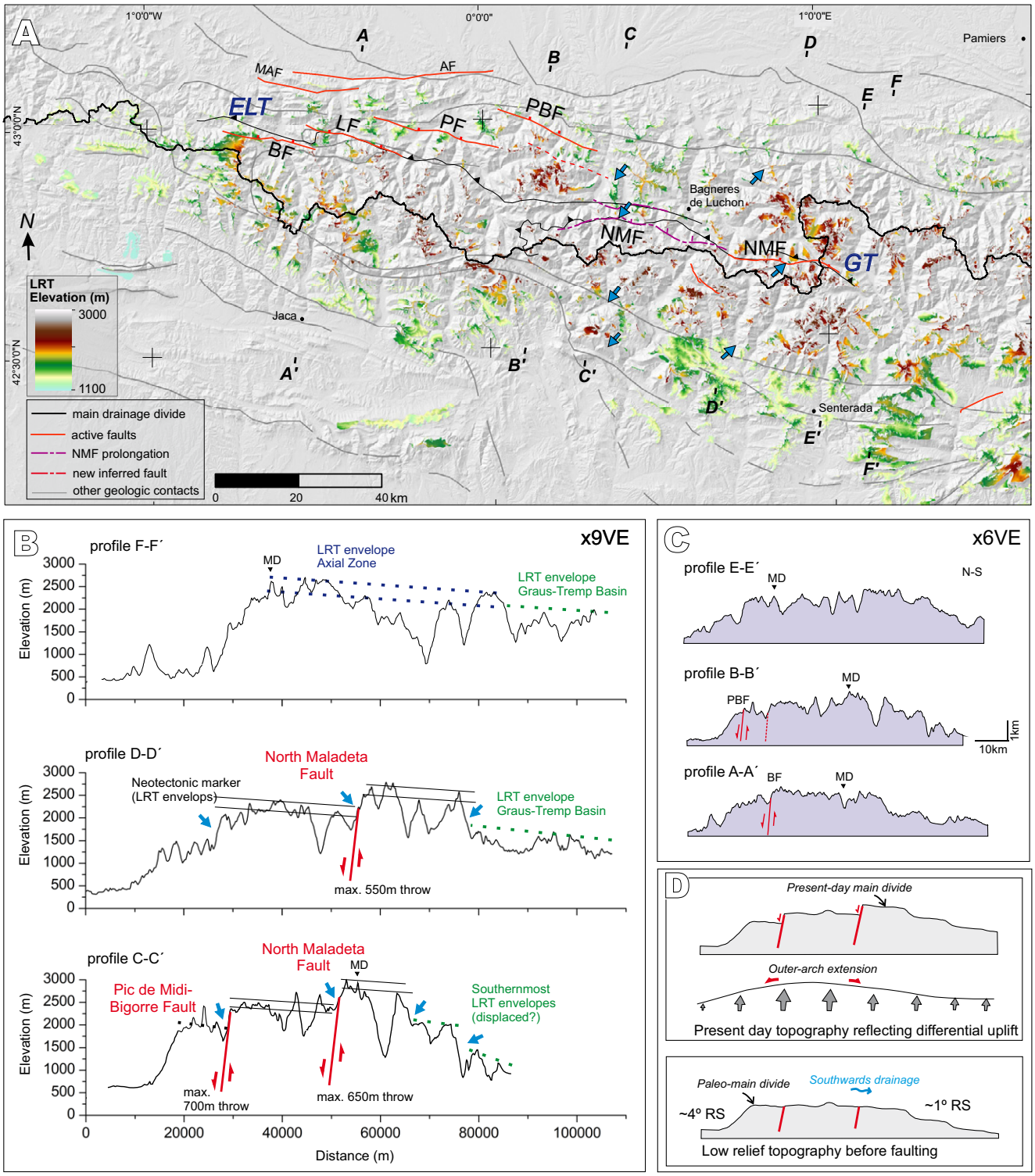

FIGURE 4. A) Shaded relief map (60m-DEM) of the Central-Western Pyrenees displaying elevation of the Low Relief Topography (LRT) remnants and some of the main tectonic structures referred in the text. Location of the ends of the long topographic profiles is indicated. B) Three of the long topographic profiles across the chain are shown with larger detail including the estimated fault throws. The envelopes of the LRT remnants are indicated with solid black lines (upper and lower envelopes) or with discontinuous green and blue lines (upper envelopes). x9VE: 9x zoom vertical scale. C) Three of the long topographic profiles across the chain are shown with less detail. x6VE: 6x zoom vertical scale. D) Sketch with the present-day topography (upper part) and the restoration of the motion of the active faults, under the assumption of regional uplift (lower part). The variations of uplift across the chain are indicated with grey arrows. A continuous slope and a smaller-than-today slope gradient are obtained in the southern Pyrenean flank. AF: Adour Fault; BF: Bedous Fault; ELC: EauxChaudes-Lakhoura Thrust; GT: Gavarnie Thrust; LF: Laruns Fault; MAF: Mail-Arrouy Fault; MD: position of the present-day Main-Drainage divide; NMF: North Maladeta Fault; PBF: Pic du Midi de Bigorre; PF: Pierrefitte Fault. The blue arrows in A) and B) indicate the position of the larger steps in LRT elevation.

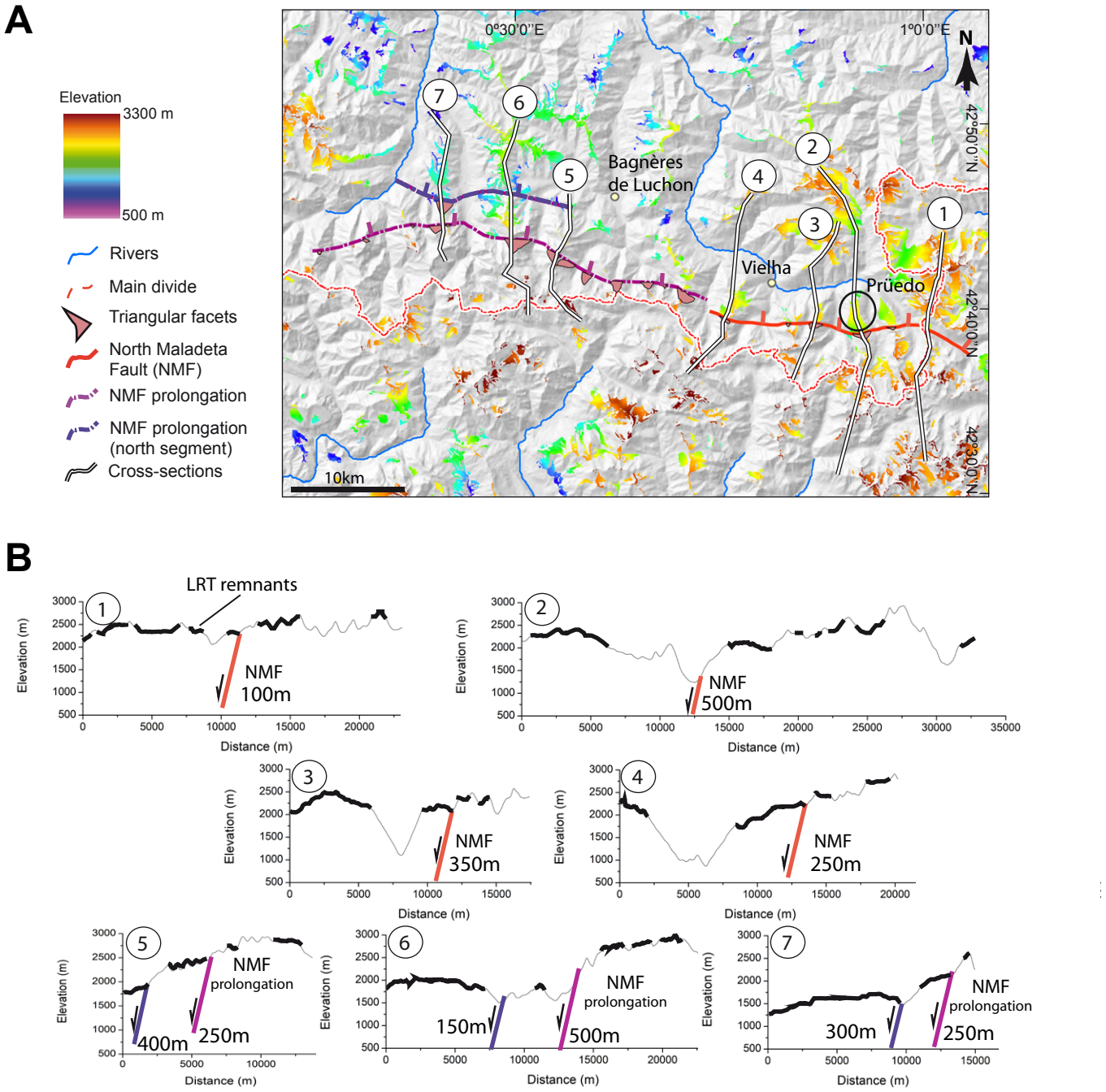

FIGURE 5. A) Shaded relief map (60m-DEM) with the revised trace of the North Maladeta Fault. It includes the elevation of the Low Relief Topography (LRT) remnants and the identified triangular facets (in black). B) Topographic profiles across the North Maladeta Fault with the LRT remnants marked in black bold lines. The maximum inferred fault throw is written next to the active fault branches, marked with red bold lines.

on the southern flank of the Pyrenees. A relatively low proportion (~12%) of the LRT polygons selected by the automatic procedure was rejected because a crosscheck with the BRGM-IGME (2009) map showed that these polygons can be interpreted as Quaternary landforms. An example of this crosscheck is given in the Figure II. In general, these overlaps correspond to glacial cirques and flat Quaternary valley bottoms located over 1,200m.

The LRT were analyzed according to their altitude, slope and relief (Figs. 3; 4), the lithology on top of which they developed, and their distribution with respect to active tectonic structures (Figs. 4; 5; I). The LRT remnants in the study area are located between 1,200 and 3,000m. The decrease in their altitude height towards the flanks is not gradual but rather shows abrupt changes, which are detailed in the next section. A distinction among the LRT remnants

mapped can be made in terms of their local relief, which reaches 350m but in most cases is <<200m. However, on the southern flank, the relief is especially low in several parts, such as at the southern boundary of the Jaca Basin or to the South of the Axial Zone southern boundary, in the interfluvial areas between the Cinca and Segre rivers (Figs. 1; 3A). These cases correspond to sites where low resistant lithologies (Cretaceous rocks and post-middle Eocene sediments) crop out and at some specific localities where the LRT remnants do not bevel the tectonic structure, such as: i) several LRT remnants on the southern flank of the Pyrenees, which correspond to depositional surfaces of Oligocene alluvial fans, such as those in the surroundings of the town of Senterada (Figs. 1; I); ii) everal structural surfaces along the large tilted panels of Cretaceous and lower Eocene carbonates at the Cadí and Montsec thrusts (Figs. 1; 2; I).

Steps in altitude distribution and revision of the North Maladeta Fault trace

Topographic profiles (Figs. 4; 5) and 3D visualizations (Fig. 6) across the study area showed that the highest LRT remnants (height >>2,000m) are concentrated in the Pyrenean Axial Zone (Fig. 4). The remnants can be constrained between two approximate envelopes (upper and lower). These envelopes, defined over the incised topography, display several marked steps in altitude. A central profile (D–D' in Fig. 4A, B) shows three steps in altitude range. The northernmost one seems to be related to the northern limit of an alignment of basement massifs, (Fig. 4A). The middle steps correspond to the North Maladeta Fault, and the southernmost step, to the southern limit of the Axial Zone. These last two steps show lateral continuity along the E-W fringes. In the profile C–C', four steps can be recognized. The two northern steps correspond to the Pic de Midi de Bigorre Fault and to the North Maladeta Fault, respectively. The other southern segments approximately match the southern limit of the Axial Zone and an alpine thrust within the South Pyrenean Zone (Fig. 4A).

Although many of the highest LRTs have developed on crystalline massifs, the surfaces are not restricted to them. A lithological control of the step-in-height only seems related to erodibility in a few cases, such as the eastern margins of the Maladeta crystalline massif (Noguera Pallaresa drainage basin) or the northeast and southeast of the Cauterets crystalline massif, which show a gradual decrease in height towards the surrounding metasediments (Figs. 1; I).

A close view of the area North of the main divide shows the characteristic altitude distribution of the LRT on both sides of the previously studied active faults (Figs. 1; 4A; 5A). The upper and lower envelopes have

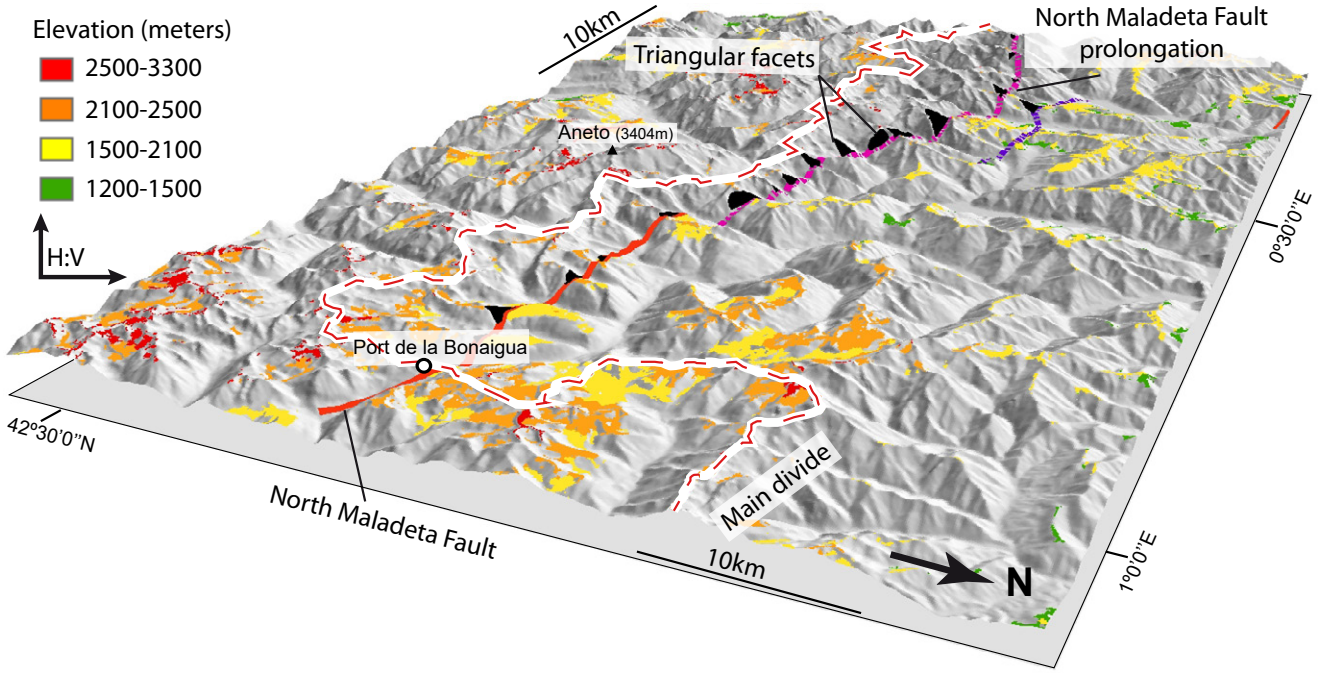

FIGURE 6. Shaded relief 3D view of the present-day topography with the elevation of the Low Relief Topography (LRT) remnants just where the main-drainage divide presents its larger offset. The North Maladeta Fault, its western prolongation and the triangular facets have been indicated. Note that the LRT elevations in the hangingwall of this fault are lower than in the footwall.

been used as neotectonic markers because they show similar characteristics; the envelopes show a slight slope to the South (~1º), that is quite constant across the whole area (Fig. 4B), and they are vertically separated by ~250–300m on both sides of the faults. However, the surfaces included in these envelopes show differences on the two sides of the faults: LRT remnants are better preserved and broader in the northern fault block. This variation could be related to the fact that in the southern fault blocks (footwalls, headwaters of the mountain range) the erosion is more ubiquitous and glacial cirques are located there, whereas in the northern blocks (hanginwalls) the erosion is concentrated along the main valleys.

The northern altitudinal steps in the LRT remnants coincide rather well with the trace of the active faults mapped previously by Lacan (2008), Ortuño *et al*. (2008; 2013) and Dumont *et al*. (2015). These are the North Maladeta fault, local reactivation of the Gavarnie Thrust, and the Bedous-Pic de Midi-Bigorre set of faults, made offour *en echelon* faults (Bedous, Laruns, Pierrefitte, Pic de Midi de Bigorre), some of them reactivated segments of the Eaux Chaudes-Lakhoura Thrust (Fig. 4A; Labaume *et al*., 2018). The marked steps in the heights of the LRT remnants approximately follow the trace of these thrusts. However, it is noteworthy that the trace of these two thrusts are locally folded. The reactivation seems to have produced short cuts and, in some places, the new fault crops out along different, straighter traces.

Among these steps, the southernmost one corresponds to the North Maladeta Fault. It can be followed for ~70km, 35km westwards of the previously mapped trace, defined in Ortuño *et al*. (2013). Other faults can be inferred between the two fault systems already described in the literature, and could correspond to the eastern prolongation of the Pierrefitte Fault and to a secondary branch of the North Maladeta Fault on the Neste river headwaters (Fig. 4A). The maps shown in Figures 4A and 5A should be taken as preliminary, since the trace was delineated by analyzing digital topography and satellite orthophotos only, and no field reconnaissance was conducted along the fault trace. Only the new identified western prolongation of the North Maladeta Fault was briefly crosschecked in the field (Fig. 2E, F). A set of triangular facets was detected along the North Maladeta Fault western prolongation. The steepness of these facets led us to consider that the LRT envelopes located on the two sides of the fault are the same marker, rather than two different LRT generations (Figs. 5A; 6). From the resulting cartography, we propose that the studied faults are part of a single, major fault system, which could be referred to as the Maladeta-Bedous Fault System (~150km in Figs. 1; 4A; 5A).

Variations in fault throw

The topographic profiles perpendicular to the fault traces were analyzed to estimate their throw after the LRT formation. We obtained 5 profiles along the Maladeta-Bedous Fault System (Figs. 4A, B, C; I; III) and 7 profiles along the North Maladeta Fault (Fig. 5).

The analysis of the profiles obtained with the mapped LRT suggests that the North Maladeta Fault is controlling their altitude distribution, separating patches located at 2,550–2,700m from other patches located at 2,200–2,250m. The vertical separation along the North Maladeta Fault reaches 500m, in agreement with previously published values (Ortuño *et al*., 2008, 2013; profile 2 in Figs. 1; 5). Ortuño *et al*. (2013) found that locally, the total throw can be larger than the topographic throw. This is because near the fault trace in the Prüedo plains (Fig. 4) the marker is affected by secondary faults and is located 100m-below the surface. The Bedous-Pic de Midi de Bigorre set of faults separates LRT remnants located at 2,800–2,600m (southern block) from other remnants located at 1,800–2,000m (northern block), as seen in profile B–B' (Figs. 1; 4A, B, C).

The overall view of the Maladeta-Bedous Fault System suggests that these faults could be part of a major fault system aligned along ~150km. The maximum summed throw of the major system is observed along a central transect (C–C' in Fig. 4A, B) and reaches 1350m.

Restoration of motion and inference of the paleo-main-drainage divide position preceding deformation

In the Central-Western Pyrenees, the orientation of the present-day main-drainage divide shows a parallelism with the orientation of the studied faults in the northern flank. That is, the segment showing a southern shifted position that starts with an abrupt kink in the eastern tip of the North Maladeta Fault and from there to the West, is nearly parallel to this fault (4–10km South of it) and to the Bedous-Pic de Midi de Bigorre set of faults (8–32km South of it, Figs. 1; 4).

We performed a simple restoration of the motion along the studied active faults (Fig. 5) that only accounts for vertical displacements and assumes faults are planar and non-rotational. We did not account for a possible tilt of the hanging-wall blocks, which in fact should be expected. The fault dip is assumed to be ~65º to the N or NE, which is based on sub-surface fault geometry deduced by Ortuño *et al*. (2008, 2013) for the North Maladeta Fault and inferred from magnetotelluric profiles. It is also in agreement with structural analysis and in-depth projection of microseismic events published by Dumont *et al*. (2015) referring to the Eaux-Chaudes-Lakhoura Thrust reactivation.

To gain a better knowledge of the fault geometry it would be necessary to carry out a better characterization of the displaced preserved geomorphological markers. In addition, this geometry could be better inferred from other types of sub-surface data as well as a robust structural analysis of rocks cropping out on both sides of the fault, which would require discriminating between variscan, alpine and post-orogenic deformations.

To explore possible regional paleo-slopes derived from different relative movements, we have considered two possible restorations by: i) fixing the fault northern blocks and considering the uplift of the fault southern blocks (option I, Fig. 4A) and; ii) fixing the fault southern block and considering the subsidence of the fault northern block (option II). These two restorations need to consider that the uplift or subsidence/collapse affects the whole chain. In the first case, regional uplift is enhanced in the central-northern part of the chain (the Axial Zone), which leads to outer arch extension, facilitating normal faulting (Fig. 4D). The increase of uplift towards the central parts of the chain and larger in the Ebro than in the Aquitanian foreland, is expected assuming that the uplift is mainly driven by erosive unloading, as discussed in several studies (*e.g.* Coney *et al.*, 1996; Gibson *et al.*, 2007; Genti *et al.*, 2016). The second option refers to gravitational collapse with absence of uplift.

The two options explored lead to similar results in terms of paleo-drainage location, which would be located between 20 and 25km to the North of the present-day divide and broadly rectilinear and continuous with respect to the segments out of the southern switch of its trace (Figs. 4D; 7). This location corresponds to a fringe approximately located at the North Pyrenean Zone (Fig. 1). In both cases, there is a strong asymmetric profile of the chain, with a ~100–120km-long southern flank against a ~30km-long northern flank at a central profile. The main differences are found in the restored paleo-slopes of the flanks compared with the present-day observed paleo-gradients, ~2.5º on the southern flank and ~4º on the northern one. These values are calculated with respect to the lower parts of the mountain flanks, marked by the uppermost alluvial deposits predating the fluvial incision (Oligocene on the southern flank and Miocene on the northern flank). On the northern flank, these reach maximum altitudes near ~500m in the Aquitanian Basin (*e.g.* Rougier *et al.*, 2016) and on the southern flank, the uppermost deposits reach almost 1,500m (*e.g.* Oligocene conglomerates, near the town of Senterada in Fig. 4A; Beamud *et al.*, 2011). The option with uplift of the southern block (option I in Fig. 4D) leads to paleo-altitudes in the center of the profile ~1,000m lower than that observed today. The retrodeformation of the uplift of the inner blocks allows us to trace a surface envelope in the studied transect that connects the northern flank LRT remnants (such as those in the Aran valley) with the southern flank remnants along a continuous ramp (paleo-Pyrenean southern flank) with a paleo-gradient of ~1º (Fig. 4D). The northern paleo-gradient would have been similar to the present-day one (~4º). The opposite restoration, with relative subsidence of the northern fault blocks results in paleo-gradients of the southern and northern paleo-flanks higher than the present-day ones. The obtained topography has a ~2º lower paleo-gradient for the southern flank, and a paleo-gradient of ~6º for the northern flank. In this case, the existence of other tectonic structures bounding the northern fault block to the North (perhaps along the North Pyrenean Fault) is necessary to facilitate the subsidence with respect to the Aquitanian Basin.

The restoration was carried out considering the 5 profiles showed in Figures 4 and III. In most of the long profiles and locally, some short profiles (as shorter profiles 3 and 6 in Fig. 5), option I results in a continuous regional topographic slope to the South.

DISCUSSION

Approach to LRT mapping

The method followed here for analyzing the low gradient topography of the Central-Western Pyrenees differs from that presented in other publications and leads to a wider portion of the present land-surface being selected as paleic surface. We use a less restrictive definition that not only considers sub-horizontal surfaces but surfaces up to 20º. In the maps of Monod *et al.* (2016), the slope range considered is very low (<10º). Consequently, areas with a larger slope but clearly showing a smooth and not incised relief are not considered, such as the summits around the Beret plain and Liat valley (Figs. 1; 2). In the cartography presented by Bosch (2016), the land surface is selected by using a parameter related to the deviation of each cell from the mean elevation, and only surfaces >1,000m are considered to perform the best fit with a comparison with hand-mapped surfaces. The main differences with respect to our method is that i) we perform cross-checking with regional and unified maps of Quaternary landforms (such as that of BRGM-IGME, 2009) as the basis for discarding the most recent surface landforms; ii) the old depositional surfaces are included, such as those mantling the southern flanks (Figs. 3; 4A) and iii) the surfaces are analyzed taking into consideration the displacement of the remnants along the active faults in the region. The BRGM-IGME (2009) map does not consider a large proportion of the LRT remnants included here. In most cases, these areas correspond to polygons mapped as "drainage divide" in the BRGM-IGME (2009) map.

Changes in the main-drainage divide

One way to cross-check the validity of the northern location of the main-drainage divide during the LRT generation in the Central-Western Pyrenees is by reviewing the provenance of the sedimentary record of the erosion and the exhumation histories proposed for the Axial Zone for the time period suspected for the LRT generation, which should be Oligocene-Miocene (post main compression and pre-late Miocene according to Ortuño *et al*., 2013). This is possible because the dismantling of the paleo-southern flank is partially recorded in alluvial fans analyzed in previous works (*e.g*. Coney *et al*., 1996; Vincent, 2001; Beamud *et al*., 2003, 2011; Michael *et al*., 2014; Roigé *et al*., 2017). In these works, middle to upper Eocene-upper Oligocene thick synorogenic conglomerate successions located within the South flank of the Pyrenees (Sis, Gurb, Canciás, Santa Orosia, Peña Oroel; Fig. 7) have been interpreted as alluvial fans deposited in the Graus-Tremp and Ainsa-Jaca piggy-back basins. Recent works (Michael *et al*., 2014; Roigé *et al*., 2017) suggest that these alluvial fans were fed by sediments that probably came from the North Pyrenean Zone. Michael *et al*. (2014) delimitated the catchments acting as source regions for the Sis and Gurb conglomerates using an ensemble of provenance tools, such as U-Pb geochronology of detrital zircons, heavy mineral analysis and clast lithology analysis. Based on these analyses, these authors placed the main divide during the middle-late Eocene ~25km North of the present-day main divide (Fig. 7).

In the Canciás, Santa Orosia, Peña Oroel alluvial fans (Fig. 7), Roigé *et al*. (2017) reported clasts of diagnostic lithologies that are only found at present-day in a narrow fringe within the North Pyrenean Zone, which is, to the North of the North Pyrenean Fault (Fig. 1). These lithologies are characteristic of the Upper Cretaceous Rift that developed in that area and was filled by breccias (the Barrandoa breccia) and grey and black flysch with interlayered volcanics. According to structural reconstructions across the area published by Teixell *et al*. (2016), these materials (or their continuation in now-eroded materials) were never located South of the northern boundary of the Axial Zone, *i.e*. South of the Bedous-Pic de Midi de Bigorre set of faults. Although this boundary could have been located to the South of the North Pyrenean Fault at some time before the end of the alpine contraction, the vertical orientation of the structures there suggests this difference was only a few kilometers.

These data lead us to locate the main paleo-divide in the middle-late Eocene at ~35km North of the present-day location. Later migration of the divide towards its present relative position, with respect to the flanks of the range, would have been influenced by the activity of the vertical faults of the Maladeta-Bedous Fault System. We envisage that without this activity and only under the influence of fluvial incision, the main-drainage divide would be at ~20km to the North of its present-day location (Fig. 7). It is not possible to determine whether this change in location occurred as a progressive migration or as a sudden jump. A progressive southward movement could have occurred by continuous fluvial advance of the paleo-headwaters of the Neste and Garona rivers, enhanced by the tectonic activity.

The onset of the fault activity and the southward movement of the main-drainage divide in the headwaters of the Neste river would have implied an increase in local slope. As a result, an increase in the river capacity is expected to have occurred, which could be related to the degradation of the LRT in that area and the onset of the Lannemezan alluvial megafan (Fig. 1). According to Mouchené *et al*. (2017) this megafan was onset at the early Miocene. The study of the influence of the activity of the newly identified North Maladeta Fault prolongation and this megafan is only preliminary and needs be better explored and supported by field research. The finding of robust evidence for this relationship could provide a reference age for the onset of the fault activity, which has never been determined. The Prüedo Basin formed during the late Miocene on top of the LRT (Fig. 5A; Ortuño *et al*., 2013) as a tectonic basin whose activity probably started some hundred thousand to millions of years before. This has to do with the accommodation space, considering the preserved thickness of these deposits (~100m, Ortuño *et al*., 2013) and the time needed to generate it. The fault segment bounding these deposits could have been already active, for instance, in the early Miocene, when the Lannemezan megafan was onset, although not necessarily so early. The Prüedo Basin is located in the westernmost tip of the North Maladeta Fault. Assuming that these two features are related to the fault activity, the younger age of the Prüedo Basin with respect to the Lannemezan megafan could also reflect the time span of fault propagation from the center towards the tips of its present-day trace, which might have an associated delay of several million years.

Origin of the elevated peneplains in the Pyrenees: unsolved controversy

Our results showed that no large, planar, sub-horizontal relief, like that identified in some areas of the Eastern Pyrenees, has been preserved in the Central-Western Pyrenees. The LRT remnants in the study area are smaller and more varied in height and slope (Figs. 3; 4A). The upper and lower envelopes of the LRT remnants analyzed separately on the two sides of the Maladeta-Bedous Fault System, show an altitude difference as high as 300m. On this basis, we can conclude that the remnants, although they are locally modified (reduced in height and with variable

slopes) with respect to an original smoother older paleo-surface, belong to: i) different generations of LRT or; ii) are part of a moderate to low relief, perhaps implying that the surface was never as planar as in the Eastern Pyrenees. Whichever way they were completed (by multi or single LRT generation), we consider that the LRT remnants on both sides of the Maladeta-Bedous Fault System are still valid for building a synthetic surface useful as a neotectonic marker.

The age of the tectonic marker used here cannot be well determined with the available data, and we can only assign to it a rough Oligocene-Miocene age. A general overview of the previously published apatite (U-Th)/He exhumation ages of the plutonic massifs in the Central-Western Pyrenees (Gibson *et al.*, 2007; Jolivet *et al.*, 2007; Metcalf *et al.*, 2009; Bosch *et al.*, 2016b; Mouchené, 2016) allows us to infer that the LRT could have been generated asynchronically. These ages (dating the time when the sample crossed the isochron for (U-Th)/He re-setting, which occurs at 40–60ºC) can be considered approximate maximum ages of surface completion. Depending on the temperature gradient and erosion rate, the delay might be of several million years. The (U-Th)/He data suggest surface completion could have been older in the North (Eocene-Oligocene) and younger (middle-late Miocene) towards the South. After their completion, it is likely that some of these landforms persisted in the landscape as inherited features. Although an incision in the LRT could have occurred locally during the Miocene, the end of surface completion probably took place during the Miocene-Pliocene, and certainly before the Quaternary. A generalized post-orogenic rejuvenation of the Pyrenean drainage is attributed to the global switch to a more contrasted and wetter climate during Quaternary times (Jones *et al.*, 1999; Lynn, 2005; Babault *et al.*, 2005, 2013; Stange *et al.*, 2013, 2014a). This would be in accordance with the late Miocene (11.1–8.7Ma) being a minimum age of the LRT in the Aran valley, as proposed by Ortuño *et al.* (2013). This age constraint is given by the age of the pollinic assemblage of the deposits of Prüedo, formed on top of the remnants (Fig. 5).

The set of data presented and discussed here supports the existence of a Pyrenean paleo-topography in which LRT remnants located now to the North of the divide in the Central-Western Pyrenees would have formed as part of a large (as large as ~100–120km-long) paleo-southern flank. The most relevant data supporting this configuration are: i) the distribution of the altitudes of the LRT remnants with respect to active faults and the main-drainage divide; ii) the topography resulting from the most reliable restoration of the fault motion, and which implies uplift of the core of the Pyrenees and iii) the provenance data of southern Oligocene conglomerates analyzed by Roigé *et al.* (2017), from which a paleo-

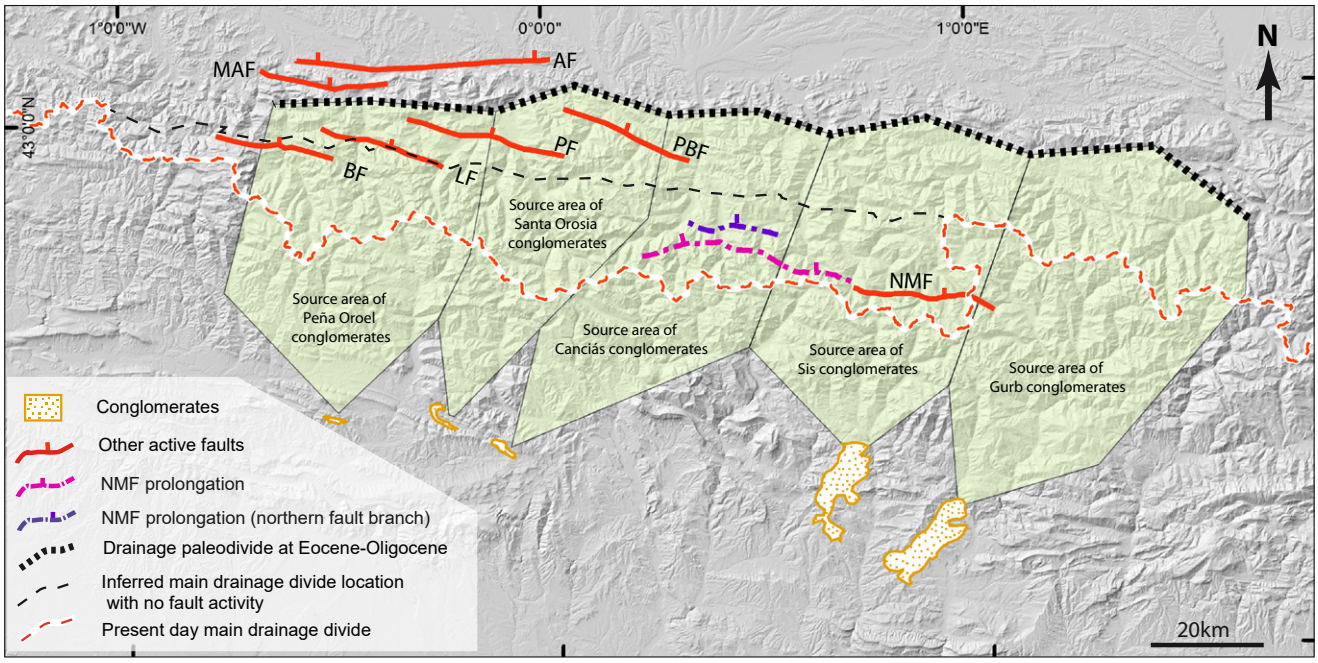

FIGURE 7. Sketch showing the estimated location of the paleo-main-drainage divide during the deposition of the upper Eocene-Oligocene conglomerates of Gurb, Sis, Canciás, Santa Orosia and Peña Oroel. Dotted lines: boundaries of the fluvial/alluvial-drainage basins according to Michael *et al.* (2014) and Roigé *et al.* (2017). The location where main divide should be at present-day with no fault activity is also marked approximately. AF: Adour fault; BF: Bedous Fault; LF: Laruns Fault; PF: Pierrefitte Fault; MAF: Mail-Arrouy Fault; NMF: North Maladeta Fault; PBF: Pic du Midi de Bigorre Fault.

main divide located North of the Axial Zone is inferred. These remnants were therefore located at the headwaters of drainage systems connected to a high paleo-base level in the Ebro Basin. The original regional paleo-slope of this drainage system would have been later disrupted by the enhanced uplift (~500m with respect to fixed foreland basins) of the central area of the Axial Zone, where the main divide is in the present-day. The kinematic feasibility of the proposed model only seems possible under regional uplift, that is, uplift that also affects the flanks and perhaps the foreland basins. This landscape evolution represents a rapprochement of the two previous proposals to explain the generation of paleic low relief in the Pyrenees (raised peneplain and raised baselevel). This "mixed model" suggests that part of the low relief of the Pyrenees was connected to a high base level located at the Ebro foreland (*i.e. raised base level model*) and would have been partially disrupted and uplifted (*i.e. raised peneplain model*). The model can be understood as a new version of the *raised base level model* that implies that preservation of LRT remnants and does not preclude the absence of a recent uplift.

The post-orogenic uplift of the central area of the Pyrenees suggested by the observations made here fits with independent data on recent uplift in the Central-Western Pyrenees found in several studies using two main approaches and discussing: i) paleo-altitudinal changes in several localities of the Axial Zone, ranging from 700 to 1,200m, as determined from the paleo-flora of the Upper Miocene deposits of the Central Pyrenees (Ortuño *et al*., 2013) and Plio-Plesitocene deposits in the western Pyrenees (Vanara *et al*., 1997); ii) uplift inferred from fluvial dynamics; the studies of Stange *et al*. (2013, 2014a, b), Victoriano *et al*. (2016) and Lewis *et al*. (2017) considered that the architecture of fluvial middle and late Quaternary stair-case terraces observed in various northern and southern Pyrenean rivers result partially from recent uplift. In particular, Lewis *et al*. (2017) obtained paleo-river profiles for the last 1Ma from which a near-uniform uplift rate is deduced.

These data are supported by recent numerical models that explore the recent uplift of the Ebro Basin and the Pyrenees as a response to erosive unloading. This uplift reaches 630m in the center of the Ebro Basin according to the erosive unloading following the Ebro-Mediterranean connection 7.5–12Ma ago (Garcia-Castellanos and Larrasoaña, 2015). The isostatic response to Quaternary differences in erosion and sedimentation across the chain was calculated by Vernant *et al*. (2013) and Genti *et al*. (2016), who obtained models supporting uplift of the central part of the Pyrenees, feasible even when slow convergence is considered and in agreement with the observed faulting mechanisms.

The geodetic studies (Asensio *et al*., 2012; Rigo *et al*., 2016; Nguyen *et al*., 2016) indicate that the Pyrenees are undergoing slow horizontal extension, reaching 4 nanostrains/yr in the western part of the chain with no detectable vertical deformation exceeding ±0.3mm/yr.

CONCLUSIONS

Models for the origin and preservation of LRT remnants and for fluvial-drainage evolution in any orogenic mountain should consider the amount of vertical displacement associated with structures active in post-orogenic times. We present the map of LRT remnants preserved in the Central-Western Pyrenees and analyze their altitude and relief distribution with respect to previously mapped and newly identified active faults. The North Maladeta Fault, previously mapped as 30km long, seems to continue along ~35km to the West, as attested by the presence of the triangular facets associated with a persistent vertical offset in the height of the LRT remnants. Its geomorphological expression is clear and follows approximately the Gavarnie thrust trace. This new western prolongation implies a new fault length (almost twice the previous estimation) for the North Maladeta Fault (~75km). This structure and another two parallel faults seem to connect two groups of faults with similar characteristics that are arranged along the Maladeta-Bedous Fault System (~150km-long), which shows accumulated throws as large as ~1350m.

We propose that the activity of the Maladeta-Bedous Fault System has influenced the position of the present-day drainage divide of the Pyrenees, explaining its marked indention towards the South in the Central-Western Pyrenees. The direct relation of the orientation of the present-day main-drainage divide with the traces of the Maladeta-Bedous Fault System and the restoration of the motion apparently experienced by the LRT remnants suggest that the paleo-drainage divide was at >>15km, and as far as 35km to the North of its present-day position at the time preceding the onset of faulting. We propose that the most likely motion of the studied faults is the one with a generalized uplift of the Pyrenees and enhanced uplift of the core of the range with respect to stable Aquitanian and Ebro basins. This paleo-reconstruction implies the existence of a marked N-S geometrical asymmetry of the chain, where the main divide was located near the North Pyrenean Zone, as already suggested in source-provenance studies of a middle-upper Eocene conglomeratic sequence that covers the southern flank. The retrodeformation results in a broad paleo-southern flank (up to ~100–120km-long) displaying a gentle slope and draining towards the Ebro Basin.

This paleo-reconstruction makes it possible to overcome some of the difficulties of the *raised base level model* proposed for the generation of LRT at high altitudes. It offers, for the first time, a suitable paleo-base level controlling the LRT remnants preserved to the North of the present-day main-drainage divide: the Ebro raised baselevel.

ACKNOWLEDGMENTS

Almost two decades ago, Pere Santanach first pointed to the tectonic displacement of the planar landforms in the Aran valley, one among his many contributions to Pyrenean geology. With this paper, we want to pay tribute to him. We acknowledge the help of Marta Roigé and Elisabet Beamud for their discussions on provenance data. The revisions done by Raimon Pallàs, Marc Calvet in a previous version of the manuscript and by Eduard Roca in the present paper substantially helped to improve the result of our work. Research was supported by the Institut de Recerca Geomodels and the RISKNAT Group (2017SGR126 SGR-AGAUR distinction).

REFERENCES

Arenas, C., Millán, H., Pardo, G., Pocoví, A., 2001. Ebro Basin continental sedimentation associated with late compressional Pyrenean tectonics (north-eastern Iberia): controls on basin margin fans and fluvial systems. Basin Research, 13(1), 65-89.

Asensio, E., Khazaradze, G., Echeverria, A., King, R.W., Vilajosana, I., 2012. GPS studies of active deformation in the Pyrenees. Geophysical Journal International, 190(2), 913-921. DOI: 10.1111/j.1365-246X.2012.05525.x

Babault, J., Van den Driessche, J., Bonnet, S., Castelltort, S., Crave, A., 2005. Origin of the highly elevated Pyrenean peneplain. Tectonics, 24(2), TC2010. DOI: 10.1029/2004TC001697

Babault, J., Van den Driessche, J., Teixell, A., 2011. Retro-to pro-side migration of the main-drainage divide in the Pyrenees: geologic and geomorphological evidence. Vienna, Austria, European Geosciences Union General Assembly 2011, April 2011, 13, EGU2011-12567.

Babault, J., Teixell, A., Struth, L., Van Den Driessche, J., Arboleya, M.L., Tesón, E., 2013. Shortening, structural relief and drainage evolution in inverted rifts: insights from the Atlas Mountains, the Eastern Cordillera of Colombia and the Pyrenees. The Geological Society of London, 377(1, Special Publications), 141-158.

Barrere, P., 1962. Relief murs perchés de la Navarre orientale. Revue géographique des Pyrénées et du Sud-Ouest. Sud-Ouest Européen, 33(4), 309-323.

Beamud, E., Garcés, M., Cabrera, L., Muñoz, J.A., Almar, Y., 2003. A new middle to late Eocene continental chronostratigraphy from NE Spain. Earth and Planetary Science Letters, 216(4), 501-514.

Beamud, E., Muñoz, J.A., Fitzgerald, P.G., Baldwin, S.L., Garcés, M., Cabrera, L., Metcalf, J.R., 2011. Magnetostratigraphy and detrital apatite fission track thermochronology in syntectonic conglomerates: constraints on the exhumation of the South-Central Pyrenees. Basin Research, 23(3), 309-331.

Beaumont, C., Muñoz, J.A., Hamilton, J., Fullsack, P., 2000. Factors controlling the Alpine evolution of the central Pyrenees inferred from a comparison of observations and geodynamical models. Journal of Geophysical Research: Solid Earth, 105(B4), 8121-8145.

Birot, P., 1937. Recherches sur la morphologie des Pyrénées orientales franco-espagnoles. PhD Thesis. Paris, J.-B. Baillière et fils, 318pp.

Boissevain, H., 1934. Étude géologique et géomorphologique d'une partie de la haute vellée du Sègre (Pyrénées catalanes). Bulletin de la Société d'histoire naturelle de Toulouse. Toulouse, LXVI, 32-170.

Bosch, G.V., 2016. Pénéplanation et dynamique de la lithosphère dans les Pyrénées. PhD Thesis. Français, Université de Rennes, 193pp.

Bosch, G.V., Van den Driessche, J., Babault, J., Robert, A., Carballo, A., Le Carlier, C., Loget, N., Prognon, C., Wyns, R., Baudin, T., 2016a. Peneplanation and lithosphere dynamics in the Pyrenees. Comptes Rendus Géoscience, 348(3-4), 194-202.

Bosch, G.V., Teixell, A., Jolivet, M., Labaume, P., Stockli, D., Domenech, M., Monie, P., 2016b. Timing of Eocene–Miocene thrust activity in the Western Axial Zone and Chaînons Béarnais (west-central Pyrenees) revealed by multi-method thermochronology. Comptes Rendus Géoscience, 348(3), 246-256.

BRGM (Bureau de Rescherches Géologiques et Minières), 2018. InfoTerre Portail. Website: www.infoterre.brgm.fr/viewer/MainTileForward.do

BRGM-IGME (Bureau de Rescherches Géologiques et Minières-Instituto Geológico y Minero de España), 2009. Quaternary Geological Map of the Pyrenees. 1:400,000. Coord. S. Courbouleix.

Calvet, M., 1992. Aplanissements sur calcaire et gîtes fossilifères karstiques. L'exemple des Corbières orientales. Tübinger Geographische Studien, 109, 37-43.

Calvet, M., 1996. Morphogenèse d'une montagne méditerranéenne: les Pyrénées orientales. Documents du BRGM 255. Bureau de Recherches Géologiques et Minières, Orléans, pg. 1177.

Calvet, M., 1999. Régimes des contraintes et volumes de relief dans l'est des Pyrénées. Géomorphologie: relief, processus, environnement, 5(3), 253-278.

Calvet, M., Gunnell, Y., 2008. Planar landforms as markers of denudation chronology: An inversion of East Pyrenean tectonics based on landscape and sedimentary basin analysis. In: Gallagher, K., Jones, S.J., Wainwright, J. (eds.). Landscape Evolution: Denudation, Climate and Tectonics over Different Time and Space Scales. The Geological Society of London, 296 (Special Publications), 147-166.

Calvet, M., Gunnell, Y., Farines, B., 2015. Flat-topped mountain ranges: Their global distribution and value for understanding the evolution of mountain topography. Geomorphology, 241, 255-291.

Choukroune, P., Séguret, M., 1973. Carte structurale des Pyrénées. Motpellier. 1:500,000. Editorial ELF-ERAP. Laboratoire de géologie structurale - Université des Sciences et Techniques du Languedoc.

Coney, P., Muñoz, J.A., McClay, K.R., Evenchick, C.A., 1996. Syntectonic burial and post-tectonic exhumation of the southern Pyrenees foreland fold-thrust belt. Journal of the Geological Society of London, 153(1), 9-16.

Crest, Y., 2017. Quantification de la dénudation glaciaire et postglaciaire dans l'orogène pyrénéen. Bilans comparés parmi des cirques et des petits bassins versants en contexte climatique océanique et méditerranéen à l'aide des nucléides cosmogéniques produits in-situ et de mesures topométriques sous SIG. PhD Thesis. Perpignan, Université de Perpignan, 426pp.

Davis, W.M., 1889. The Geographical Cycle. The Geographical Journal, 14(5), 481-504.

Davis, W.M., 1911. The Colorado Front Range: a study on physiographic presentation. Annals Association American Geographers, 1(1), 21-83.

De Sitter, L.U., 1952. Pliocene uplift of Tertiary mountain chains. American Journal of Science, 250(4), 297-307.

Dumont, T., Replumaz, A., Rouméjon, S., Briais, A., Rigo, A., Bouillin, J.-P., 2015. Microseismicity of the Béarn range: Reactivation of inversion and collision structures at the northern edge of the Iberian plate. Tectonics, 34(5), 934-950.

Farines, B., Calvet, M., Gunnell, Y., 2015. The summit erosion surfaces of the inner Betic Cordillera: Their value as tools for reconstructing the chronology of topographic growth in southern Spain. Geomorphology, 233, 92-111.

Fidalgo González, L., 2001. La cinématique de l'Atlantique Nord: la question de la déformation intraplaque. PhD. Thesis. Brest, Université de Bretagne Occidentale, 293pp.

Fillon, C., van der Beek, P., 2012. Post-orogenic evolution of the southern Pyrenees: constraints from inverse thermos-kinematic modelling of low-temperature thermochronology data. Basin Research, 24(4), 418-436.

Fitzgerald, P.G., Muñoz, J.A., Coney, P.J., Baldwin, S.L., 1999. Asymmetric exhumation across the Pyrenean orogen: Implications for the tectonic evolution of a collisional orogen. Earth and Planetary Science Letters, 173(3), 157-170.

Garcia-Castellanos, D., Larrasoaña, J.C., 2015. Quantifying the post-tectonic topographic evolution of closed basins: The Ebro basin (northeast Iberia). Geology, 43(8), 663-666.

García-Saínz, L., 1940. Las superficies de erosión que preceden a los glaciares cuaternarios del Pirineo Central y sus recíprocas influencias. Estudios Geográficos, 1(1), 46-73.

Gallart, J., Díaz, J., Nercessian, A., Mauffret, A., Dos Reis, T., 2001. The eastern end of the Pyrenees: seismic features at the transition to the NW Mediterranean. Geophysical Research Letters, 28(11), 2277-2280.

Genti, M., Chery, J., Vernant, P., Rigo, A., 2016. Impact of gravity forces and topography denudation on normal faulting in Central–Western Pyrenees: Insights from 2D numerical models. Comptes Rendus Geoscience, 348(3), 173-183.

Gibson, M., Sinclair, H.D., Lynnn, G.J., Stuart, F.M., 2007. Late to post-orogenic exhumation of the Central Pyrenees revealed through combined thermochronological data and modelling. Basin Research, 19(3), 323-334.

Goron, L., 1937. Les unités topographiques du Pays ariégeois: Le rôle des cycles dérosion tertiaires et des glaciations quaternaires dans leur morphologie. Revue géographique des Pyrénées et du Sud-Ouest, 8(4), 300-334.

Goudie, A.S. (ed.), 2004. Encyclopedia of Geomorphology, volume 1. London, Routledge, 1156pp [pg.: 62].

Gunnell, Y., Zeyen, H., Calvet, M., 2008. Geophysical evidence of a missing lithospheric root beneath the Eastern Pyrenees: Consequences for post-orogenic uplift and associatedgeomorphic signatures. Earth and Planetary Science Letters, 276(3-4), 302-313.

Gunnell, Y., Calvet, M., Brichau, S., Carter, A., Aguilar, J.P., Zeyen, H., 2009. Low long-term erosion rates in high-energymountain belts: Insights fromthermo- and biochronologyin the Eastern Pyrenees. Earth and Planetary Science Letters, 278(3-4), 208-218.

Hartevelt, J.J.A., 1970. Geology of the Upper Segre and Valira valleys, Central Pyrenees, Andorra/Spain. Leidse Geologische Mededelingen, 45(1), 167-236.

Hilley, G.E., Strecker, M.R., 2005. Processes of oscillatory basin filling and excavation in a tectonically active orogen: Quebrada del Toro basin, NW Argentina. Geological Society of America Bulletin, 117(7-8), 887-901.

IGME (Instituto Geológico y Minero de España), 2018. Portal Geode. Available in: www.info.igme.es/cartografiadigital/geologica/Geode.aspx

Jarman, D., Calvet, M., Corominas, J., Delmas, M., Gunnell, Y., 2014. Large-scale rock slope failures in the eastern Pyrenees: identifying a sparse but significant population in paraglacial and parafluvial contexts. Geografiska Annaler: Series A, Physical Geography, 96(3), 357-391.

Jolivet, M., Labaume, P., Monié, P., Brunel, M., Arnaud, N., Campani, M., 2007. Thermochronology constraints for the propagation sequence of the south Pyrenean basement thrust system (France-Spain). Tectonics, 26(5), TC5007. DOI: 10.1029/2006TC002080

Jones, S.J., Frostick, L.E., Astin, T.R., 1999. Climatic and tectonic controls on fluvial incision and aggradation in the Spanish Pyrenees. Journal of the Geological Society, 156(4), 761-769.

Kleinsmiede, W.F.J., 1960. Geology of the Valle de Aran (Central Pyrenees). Leidse Geologische Mededelingen, 25, 129-245.

Kooi, H., Beaumont, C., 1996. Large-scale geomorphology: Classical concepts reconciled and integrated with contemporary ideas via a surface processes model. Journal of Geophysical Research: Solid Earth, 102(B2), 3361-3386.

Labaume, P., Teixell, A., 2018. 3D structure of subsurface thrusts in the eastern Jaca Basin, southern Pyrenees. Geologica Acta, 16(4), 477-498. DOI: 10.1344/GeologicaActa2018.16.4.9

Lacan, P., 2008. Activité Sismotectonique Plio-Quaternaire de l'Ouest des Pyrénées. PhD Thesis. Pau, Université de Pau et des Pays de l'Adour, 284pp.

Lacan, P., Ortuño, M., 2012. Active Tectonics of the Pyrenees: A review. Journal of Iberian Geology, 38(1), 9-30.

Leonard, E.M., 2002. Geomorphic and tectonic forcing of late Cenozoic warping of the Colorado piedmont. Geology, 30(7), 595-598.

Lewis, C.J., Sancho, C., McDonald, E.V., Peña-Monné, J.L., Pueyo, E.L., Rhodes, E., Calle, M., Soto, R., 2017. Post-tectonic landscape evolution in NE Iberia using staircase terraces: Combined effects of uplift and climate. Geomorphology, 292(1), 85-103.

Lynn, G.J., 2005. Macrogeomorphology and erosional history of the postorogenic Pyrenean mountain belt. Doctoral Thesis. Edinburgh, University of Edinburgh, 388pp.

Meigs, A.J., Burbank, D.W., 1997. Growth of the south Pyrenean orogenic wedge. Tectonics, 16(2), 239-258.

Metcalf, J.R., Fitzgerald, P.G., Baldwin, S.L., Muñoz, J.A., 2009. Thermochronology of a convergent orogen: constraints on the timing of thrust faulting and subsequent exhumation of the Maladeta Pluton in the Central Pyrenean Axial Zone. Earth and Planetary Science Letters, 287, 488–503.

Michael, N.A., Carter, A., Whittaker, A.C., Allen, P.A., 2014. Erosion rates in the source region of an ancient sediment routing system: comparison of depositional volumes with thermochronometric estimates. Journal of the Geological Society, 171(3), 401-412.

Millán-Garrido, H.M., Morer, E.P., Cardona, M.A., Aguado, A.L., Urcia, B.O., Peña, B.M., 2000. Actividad tectónica registrada en los depósitos terciarios del frente meridional del Pirineo central. Revista de la Sociedad Geológica de España, 13(2), 279-300.

Molnar, P., England, P., 1990. Late Cenozoic uplift of mountain ranges and global climate change: chicken or egg? Nature, 346(6279), 29-34.

Monod, B., Regard, V., Carcone, J., Wyns, R., Christophoul, F., 2016. Postorogenic planar palaeosurfaces of the central Pyrenees: Weathering and neotectonic records. Comptes Rendus Géoscience, 348(3-4), 184-193.

Mouchené, M., van der Beek, P., Carretier, S., Mouthereau, F., 2017. Autogenic versus allogenic controls on the evolution of a coupled fluvial megafan-mountainous catchment system: numerical modelling and comparison with the Lannemezan megafan system (northern Pyrenees, France). Earth Surface Dynamics, 5(1), 125.

Muñoz, J.A., 1992. Evolution of a continental collision belt: ECORS-Pyrenees crustal balanced cross-section. In: McClay, K.R. (ed.). Thrust Tectonics. London, Chapman and Hall, 235-246. DOI: 10.1007/978-94-011-3066-0_21

Muñoz, J.A., 2002. Alpine tectonics I: the Alpine system north of the Betic Cordillera. Tectonic setting; The Pyrenees. In: Gibbons, W., Moreno T. (eds.). The Geology of Spain. The Geological Society of London, 370-385.

Muñoz, J.A., Mencos, J., Roca, E., Carrera, N., Gratacós, O., Ferrer, O., Fernández, O., 2018. The structure of the South-Central-Pyrenean fold and thrust belt as constrained by subsurface data. Geologica Acta, 16(4), 439-460. DOI: 10.1344/GeologicaActa2018.16.4.7

Nguyen, H.N., Vernant, P., Mazzotti, S., Khazaradze, G., Asensio, E., 2016. 3-D GPS velocity field and its implications on the present-day post-orogenic deformation of the Western Alps and Pyrenees. Solid Earth, 7(5), 1349-1363. DOI: 10.5194/se-7-1349-2016

Oliva-Urcia, B., Beamud, E., Garces, M., Arenas, C., Soto, R., Pueyo, E.L., Pardo, G., 2015. New magnetostratigraphic dating of the Palaeogene syntectonic sediments of the west-central Pyrenees: tectonostratigraphic implications. In: Pueyo, E.L., Cifelli, F., Sussman, A.J., Oliva-Urcia, B. (eds.). Palaeomagnetism in Fold and Thrust Belts: New Perspectives. The Geological Society of London, 425(1, Special Publications), 107-128.

Ollier, C.D., Pain, C.F., 2000. The Origin of Mountains. London, Routledge, 345pp.

Ortuño, M., 2008. Deformación activa en el Pirineo Central: la falla Norte de la Maladeta y otras fallas activas. PhD Thesis. Barcelona, Universitat de Barcelona, 346pp.

Ortuño, M., Queralt, P., Martì, A., Ledo, J., Masana, E., Perea, H., Santanach, P., 2008. The North Maladeta Fault (Spanish Central Pyrenees) as the Vielha 1923 earthquake seismic source: Recent activity revealed by geomorphological and geophysical research. Tectonophysics, 453(1-4), 246-262.

Ortuño, M., Martí, A., Martín-Closas, C., Jiménez-Moreno, G., Martinetto, E., Santanach, P., 2013. Palaeoenvironments of the Late Miocene Prüedo Basin: implications for the uplift of the Central Pyrenees. Journal of the Geological Society, 170(1), 79-92.

Ortuño, M., Guinau, M., Calvet, J., Furdada, G., Bordonau, J., Ruíz, A., Camafort, M., 2017. Potential of airborne LiDAR data analysis to detect subtle landforms of slope failure: Portainé (Central Pyrenees). Geomorphology, 295, 364-382.

Penck, A., 1885. La Période glaciaire dans les Pyrénées. Bulletin de la Société d'Histoire Naturelle de Toulouse, 1, 105-200.

Penck, W., 1923. Morphological Analysis of Land Forms. English translation: Czech, H., Boswell, K.C., 1953. Morphological Analysis of Land Forms. London, Macmillan and Co., 180pp.

Peña, J.L., 1983. La conca de Tremp y sierras prepirenaicas comprendidas entre les rios Segre y Noguera Ribagorzana: estudio geomorfológico. PhD Thesis. Universidad de Zaragoza. Institut d'Estudis Ilerdenses. Diputació Provincial de Lleida, 373pp. [Available in: www.dialnet.unirioja.es/servlet/libro?codigo=41652]

Phillips, J.D., 2002. Erosion, isostatic response, and themissing peneplains. Geomorphology, 45(3-4), 225-241.

Rigo, A., Vernant, P., Feigl, K.L., Goula, X., Khazaradze, G., Talaya, J., Morel, L., Nicolas, J., Baize, S., Chéry, J., Sylvander, M., 2015. Present-day deformation of the Pyrenees revealed by GPS surveying and earthquake focal mechanisms until 2011. Geophysical Journal International, 201, 947-964. DOI: 10.1093/gji/ggv052

Roca, E., 1986. Estudi geològic de la fossa de la Cerdanya. Doctoral Thesis. Barcelona, Universitat de Barcelona, 109pp.

Rodríguez Vidal J., 1983. Geomorfología de las Sierras Exteriores Oscences y su piedemonte. PhD Tesis. Zaragoza, Universidad de Zaragoza, 493pp.

Roigé, M., Gómez-Gras, D., Remacha, E., Boya, S., Viaplana-Muzas, M., Teixell, A., 2017. Recycling an uplifted early foreland basin fill: An example from the Jaca basin (Southern Pyrenees, Spain). Sedimentary Geology, 360, 1-21.

Rougier, G., Ford, M., Christophoul, F., Bader, A.G., 2016. Stratigraphic and tectonic studies in the central Aquitaine Basin, northern Pyrenees: Constraints on the subsidence and deformation history of a retro-foreland basin. Comptes Rendus Geoscience, 348(3-4), 224-235.

Rushlow, C.R., Barnes, J.B., Ehlers, T.A., Vergés, J., 2013. Exhumation of the southern Pyrenean fold-thrust belt (Spain) from orogenic growth to decay. Tectonics, 32(4), 843-860.

Sala, M., 1984. Pyrenees and Ebro Basin Complex. In: Geomorphology of Europe, Palgrave, Macmillan ed., London, 269-293.

Stange, K.M., Van Balen, R.T., Vandenberghe, J., Peña, J.L., Sancho, C., 2013. External controls on Quaternary fluvial incision and terrace formation at the Segre River, Southern Pyrenees. Tectonophysics, 602, 316-331.

Stange, K.M., Van Balen, R.T., Garcia-Castellanos, D., Cloetingh, S., 2014a. Numerical modelling of Quaternary terrace staircase formation in the Ebro foreland basin, southern Pyrenees, NE Iberia. Basin Research, 28(1), 124-146.

Stange, K.M., Van Balen, R.T., Kasse, C., Vandenberghe, J., Carcaillet, J., 2014b. Linking morphology across the glaciofluvial interface: A10Be supported chronology of glacier advances and terrace formation in the Garonne River, northern Pyrenees, France. Geomorphology, 207, 71-95.

Struth, L., Teixell, A., 2016. Dinámica fluvial en rifts invertidos a partir del parámetro χ: aplicación a la Cordillera Oriental de Colombia y a otras cordilleras de referencia. Geogaceta, 60, 55-58.

Teixell, A., 1998. Crustal structure and orogenic material budget in the west central Pyrenees. Tectonics, 17(3), 395-406.

Teixell, A., Muñoz, J.A., 2000. Evolución tectonosedimentaria del Pirineo meridional durante el Terciario: una síntesis basada en la transversal del río Noguera Ribagorçana. Revista de la Sociedad Geológica de España, 13(2), 251-264.

Teixell, A., Labaume, P., Lagabrielle, Y., 2016. The crustal evolution of the west-central Pyrenees revisited: Inferences from a new kinematic scenario. Comptes Rendus Geoscience, 348(3-4), 257-267.

Vanara, N., Maire, R., Lacroix, J., 1997. The carbonated palaeosurface of the ''Arbailles'' massif (Pyrennes-Atlantiques): An example of Neogene hydrographic network dried up by uplift and karstification. Bulletin de La Société Géologique de France, 168(6), 255-265.

Vergés, J., 1993. Estudi geològic del vessant sud del Pirineu oriental i central. Evolució cinemàtica en 3D. PhD. Thesis. Barcelona, Universitat de Barcelona, 203pp.

Vergés, J., Muñoz, J.A., 1990. Thrust sequences in the Southern Central Pyrenees. Bulletin de la Société Géologique de France, 6(2), 265-271.

Vergés, J., Burbank, D.W., 1996. Eocene-Oligocene thrusting and basin configuration in the eastern and central Pyrenees (Spain). In: Friend, P., Dabrio, C.J. (eds.). Tertiary basins of Spain: the stratigraphic record of crustal kinematics. World and Regional Geology. Cambridge, Cambridge Universtiy Press, 120-133.

Vergés, J., Millán, H., Roca, E., Muñoz, J., Marzo, M., Cirés, J., Den Bezemer, T., Zoetemeijer, R., Cloetingh, S., 1995. Eastern Pyrenees and related foreland basins: pre-, syn- and post-collisional crustal-scale cross-sections, 12(8), 903-915.

Vergés, J., Fernàndez, M., Martínez, A., 2002. The Pyrenean orogen: pre-, syn-, and post-collisional evolution. Journal of the Virtual Explorer, 8, 55-74.

Vernant, P., Hivert, F., Chéry, J., Steer, P., Cattin, R., Rigo, A., 2013. Erosion-induced isostatic rebound triggers extension in low convergent mountain ranges. Geology, 41(4), 467-470.

Victoriano, A., García-Silvestre, M., Furdada, G., Bordonau, J., 2016. Long-term entrenchment and consequences for present flood hazard in the Garona River (Val d'Aran, Central Pyrenees, Spain). Natural Hazards Earth System Sciences, 16(9), 2055-2070.

Vincent, S.J., 2001. The Sis palaeovalley: a record of proximal fluvial sedimentation and drainage basin development in response to Pyrenean mountain building. Sedimentology, 48(6), 1235-1276.

Whitchurch, A.L., Carter, A., Sinclair, H.D., Duller, R.A., Whittaker, A.C., Allen, P.A., 2011. Sediment routing system evolution within a diachronously uplifting orogen: Insights from detrital zircon thermochronological analyses from the South-Central Pyrenees. American Journal of Science, 311(5), 442-482.

Zandvliet, J., 1960. The geology of the upper Salat and Pallaresa valleys, Central Pyrenees, France/Spain. Leidse Geologische Mededelingen, 25(1), 1-127

Manuscript received February 2018;
revision accepted October 2018;
published Online December 2018.